antibiotics

MDPI

Article

Biosynthesis of Smaller-Sized Platinum Nanoparticles Using the Leaf Extract of *Combretum erythrophyllum* and Its Antibacterial Activities

Olufunto T. Fanoro [1,2], Sundararajan Parani [2,3], Rodney Maluleke [2,3], Thabang C. Lebepe [2,3], Rajendran J. Varghese [2,3], Nande Mgedle [2,3], Vuyo Mavumengwana [1] and Oluwatobi S. Oluwafemi [2,3,*]

1 Department of Biotechnology, University of Johannesburg, Doornfontein, Johannesburg 2028, South Africa; jolufunto@gmail.com (O.T.F.); vuyom@uj.ac.za (V.M.)
2 Centre for Nanomaterials Sciences Research, University of Johannesburg, Doornfontein, Johannesburg 2028, South Africa; sbarani416@gmail.com (S.P.); rodney.maluleke@gmail.com (R.M.); calvyn.tl@gmail.com (T.C.L.); josv3209@gmail.com (R.J.V.); nandemgedle@gmail.com (N.M.)
3 Department of Chemical Sciences (Formerly Applied Chemistry), University of Johannesburg, Doornfontein, Johannesburg 2028, South Africa
* Correspondence: oluwafemi.oluwatobi@gmail.com

Abstract: Nanobiotechnology is a promising field in the development of safe antibiotics to combat the increasing trend of antibiotic resistance. Nature is a vast reservoir for green materials used in the synthesis of non-toxic and environmentally friendly nano-antibiotics. We present for the first time a facile, green, cost-effective, plant-mediated synthesis of platinum nanoparticles (PtNPs) using the extract of *Combretum erythrophyllum* (CE) plant leaves. The extract of CE served as both a bio-reductant and a stabilizing agent. The as-synthesized PtNPs were characterized using ultraviolet-visible (UV–Vis) absorption spectroscopy, high-resolution transmission electron microscopy (HR-TEM), Fourier transform infrared spectroscopy (FTIR), X-ray diffraction (XRD), and dynamic light scattering (DLS) techniques. The HR-TEM image confirmed that the PtNPs are ultrasmall, spherical, and well dispersed with an average particle diameter of 1.04 ± 0.26 nm. The PtNPs showed strong antibacterial activities against pathogenic Gram-positive *Staphylococcus epidermidis* (ATCC 14990) at a minimum inhibitory concentration (MIC) of 3.125 µg/mL and Gram-negative *Klebsiella oxytoca* (ATCC 8724) and *Klebsiella aerogenes* (ATCC 27853) at an MIC value of 1.56 µg/mL. The CE-stabilized PtNPs was mostly effective in *Klebsiella* species that are causative organisms in nosocomial infections.

Keywords: *Combretum erythrophyllum*; platinum nanoparticles; green synthesis; antibacterial; *Klebsiella oxytoca*; *Klebsiella aerogenes*

Citation: Fanoro, O.T.; Parani, S.; Maluleke, R.; Lebepe, T.C.; Varghese, R.J.; Mgedle, N.; Mavumengwana, V.; Oluwafemi, O.S. Biosynthesis of Smaller-Sized Platinum Nanoparticles Using the Leaf Extract of *Combretum erythrophyllum* and Its Antibacterial Activities. *Antibiotics* **2021**, *10*, 1275. https://doi.org/10.3390/antibiotics10111275

Academic Editor: Maria Fernanda N. N. Carvalho

Received: 21 September 2021
Accepted: 16 October 2021
Published: 20 October 2021

1. Introduction

Nanobiotechnology, an emerging field of nanoscience, has advanced the development of green practices in producing bio-inspired nanoparticles (NPs). It involves using biomolecules in the production of nanomaterials and nano-based systems. These biomolecules account for the variation in the size, shape, wavelength, surface area, and functionalization of these nanoparticles [1–3]. Noble metal nanoparticles (MNPs) such as platinum, gold, and silver have been used in diverse applications such as pharmaceutics, gas sensors, electronics, medicine, diagnosis, fuel cells, sensing, drug, gene delivery, etc. This is due to their excellent intrinsic optical, electronic, and physicochemical properties, which offer them functional capabilities different from the bulk materials [2,4], giving "Ockham's razor" to applied nanomedicine because of the flexibility in their multifunctionalization in bio-applications [5]. Among the noble MNPs, platinum nanoparticles (PtNPs) possess inherent and distinct properties such as high surface area, resistance to corrosion, and biocidal effects [6]. Several physical and chemical methods have been used in the synthesis of PtNPs. However, these processes are not completely green due to the

use of high temperatures and toxic reagents. In addition, large-scale synthesis is not easy to achieve with such methods [7]. To proffer alternatives to these procedures, a benign and environmentally friendly approach has been used by prospecting microorganisms [8], plant extract [9,10], and polysaccharides [11] for the synthesis of PtNPs. Amongst these biological entities, the use of plant extracts (PE) has proved to be an excellent choice because they are readily available, simple, cost-effective, eco-friendly, and highly bio-compatible for biomedical applications [12]. Furthermore, PE contains diverse phytochemicals or metabolites such as carbohydrates, alkaloids, terpenes, phenols, tannins, lipids, quinones, reductases, proteins, flavonoids, vitamins, etc. [13–15]. Therefore, they can serve as both reducing and stabilizing agents, thus eliminating the use of hazardous chemical reagents in the synthesis of MNPs [16]. These phytochemicals or metabolites can prevent the aggregation of nanoparticles, reduce generic toxicity, and increase their bio-assimilation [4,17,18]. Several plant, leaf, flower, and seed extracts of *Taraxacum laevigatum* [9], *Garcinia mangostana* L. [19], *Xanthium strumarium* [20], *Punica granatum* [2], *Nigella sativa L.* [6], etc. have been used in the biogenic synthesis of PtNPs. Despite these, it is imperative to explore more plant sources due to their vast array of phytochemicals.

Combretum erythrophyllum (CE) is a native plant in South Africa belonging to the medicinal family of Combretaceae. It grows independently and usually serves as a shade or an ornamental plant [4,21]. Different extracts of the CE plant's leaves, bark, and seeds have been used customarily for medicinal purposes due to their richness in secondary metabolites [22]. Prior studies have shown that its leaf and extract contain flavonoids, alkaloids, phenolics, carbohydrates, proteins, and essential oils [20,22], which are excellent bio-reductants. Despite these excellent properties, there has been no known research on the use of *C. erythrophyllum* extract in the green synthesis of PtNPs or extracts from the Combretaceae family, as it has been reported for other MNPs such as silver and gold. Furthermore, as far as the authors know, there has been no report on the antibiotic properties of PtNPs synthesized using the extract of *C. erythrophyllum*. Herein, we report for the first time the synthesis of PtNPs using the aqueous extract of CE leaves as both reducing and stabilizing agents. The formation of the as-synthesized PtNPs was confirmed by using Ultraviolet-Visible (UV–Vis) absorption spectroscopy. The morphological and structural evaluation was carried out by using high-resolution transmission electron microscopy (HR-TEM). The biological activity of the as-synthesized PtNPs was evaluated using minimum inhibition concentration (MIC) for its antibacterial activity against Gram-positive and Gram-negative bacteria. The results showed that the CE-PtNPs exhibited selective antibacterial activity toward specific pathogenic *Klebsiella* species, which could serve as a means for controlling infectious diseases.

2. Results and Discussion

2.1. UV-Visible Spectra

The growth of biosynthesized PtNPs using C. *erythrophyllum extract* was monitored by observing the change in the color of the reaction mixture. As the reaction progressed, the color changed from light yellow to brown and finally darkish brown. This observed color change shows the conversion of the Pt (IV) to Pt (II) and finally to Pt (0), indicating the formation of PtNPs. The observed color change can be attributed to the surface plasmon response of MNPs due to the vibration of free electrons on its surface. The formation of PtNPs at 24 h reaction time was confirmed by UV-Vis spectroscopy. The absorption spectra of the precursor platinum (Pt) salt showed a plasmon peak at 262 nm as a result of the dissociation and formation of $2H^+$ and $PtCl_6^{2-}$ in water [19]. Nevertheless, after the reduction by the CE extract, the plasmon peak of the Pt salt disappeared, thus signifying a total reduction of the Pt salt to a zero-valent platinum (Figure 1). A similar result was reported for the biosynthesis of PtNPs using the extract of *Psidium guajava* [23].

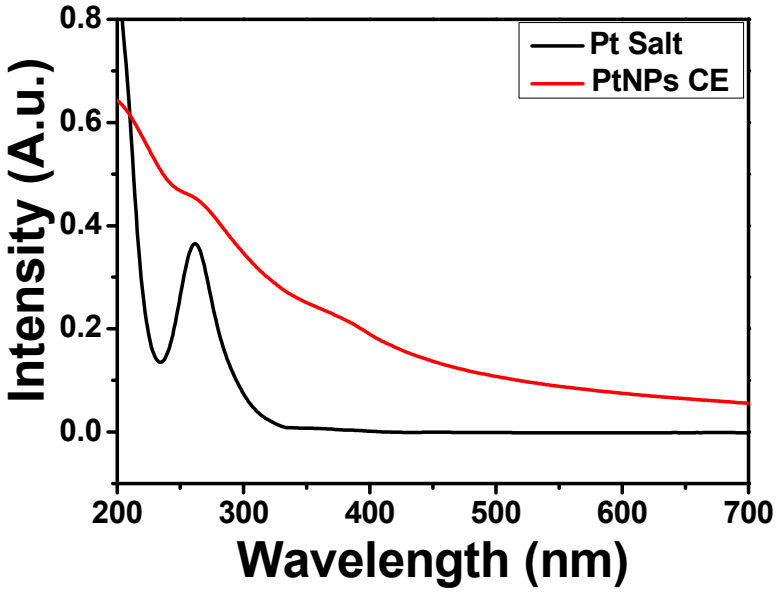

Figure 1. Absorbance spectra of platinum salt and PtNPs CE.

2.2. XRD Analysis

The XRD pattern of the CE-PtNPs at 24 h is shown in Figure 2. The diffraction pattern shows peaks at 2θ values of 39.99°, 46.49°, 67.70°, and 81.49°, corresponding to the (111), (200), (220), and (311) crystallographic planes of the face-centered cubic (*fcc*) with the lattice parameter a = 3.92 Å, which is in accordance with JCPDs-ICDD Card no: 04-802 [24]. Similar results have been reported in the biosynthesis of PtNPs using *Punica granatum* crusts extract [2]. The high intensity of the peak at 39.99° shows that the nanoparticles were predominantly oriented toward the (111) plane. The width of the (111) peak was used to calculate the average crystallite size by using the Scherrer equation [25]. The calculated average size was 1.83 nm, which is in agreement with the size obtained from the HR-TEM.

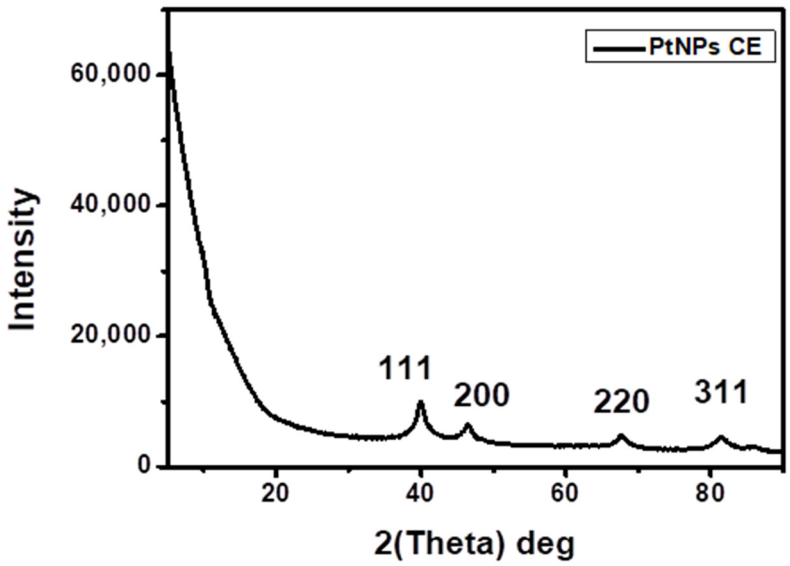

Figure 2. XRD patterns of the as-synthesized PtNPs CE.

2.3. TEM Analysis

Figure 3 shows the TEM micrograph of the as-synthesized PtNPs using the CE extract as a bio-reductant. As shown in Figure 3a, the as-prepared PtNPs are small and mostly spherical. The presence of lattice fringes in the high-resolution image indicates

the crystallinity of the PtNPs. Figure 3b shows the correlation of the calculated lattice (d) spacing values with the XRD patterns. Furthermore, the selected area electron diffraction (SAED) image shows the ring patterns accompanied by the single spots in a ring (Figure 3b inset), which are in agreement with the XRD patterns. The particle size distribution that was obtained from the TEM micrograph is shown in Figure 4a. The particle size ranged between 0.2 and 1.8 nm with an average particle diameter of 1.04 ± 0.26 nm. In Figure 4b, the energy-dispersive X-ray spectrum (EDX) showed the occurrence of Pt and elements such as calcium, oxygen, and potassium, which come from CE extract, showing its richness in minerals. The Cu is a result of the copper grid used for the analysis. The PtNPs-CE showed a negative zeta potential of −34.1 mV, signifying sufficient surface charge for electrostatic and colloidal stability in biological systems [4].

2.4. FTIR Analysis

FTIR spectroscopy was used to investigate the surface chemistry of the as-synthesized PtNPs and confirm the functional groups of the biomolecules involved in reducing and capping the as-synthesized PtNPs. The FTIR spectra of both the CE and the as-synthesized PtNPs are shown in Figure 5, with common absorption bands presented in Table 1. The major absorption bands in the PtNPs are 3283 cm^{-1}, 2920 cm^{-1}, 2850 cm^{-1}, 1708 cm^{-1}, and 1620 cm^{-1}. The peak at 3283 cm^{-1} correlates to the O-H stretching (intramolecular bonding) of the hydroxyl group found in polyphenols; peaks at 2920 cm^{-1} and 2850 cm^{-1} are attributed to the asymmetric stretch of C-H group of alkanes. The peak at 1708 cm^{-1} is attributed to the C=O stretching found in typical flavonoids or flavones. The peak at 1620 cm^{-1} correlates to the carboxylate anion stretching (-COO-) of proteins and amino acids. The shift observed in the wavenumber of -OH, C-H, C=O, and -COO- stretching of PtNPs compared to the CE extract shows possible coordination between the PtNPs and the CE extract [26]. Thus, it is believed that the proteins, flavonoids, amino acids, polyphenols, and carbohydrates biomolecules present in CE served as both bio-reductant and stabilizing agents.

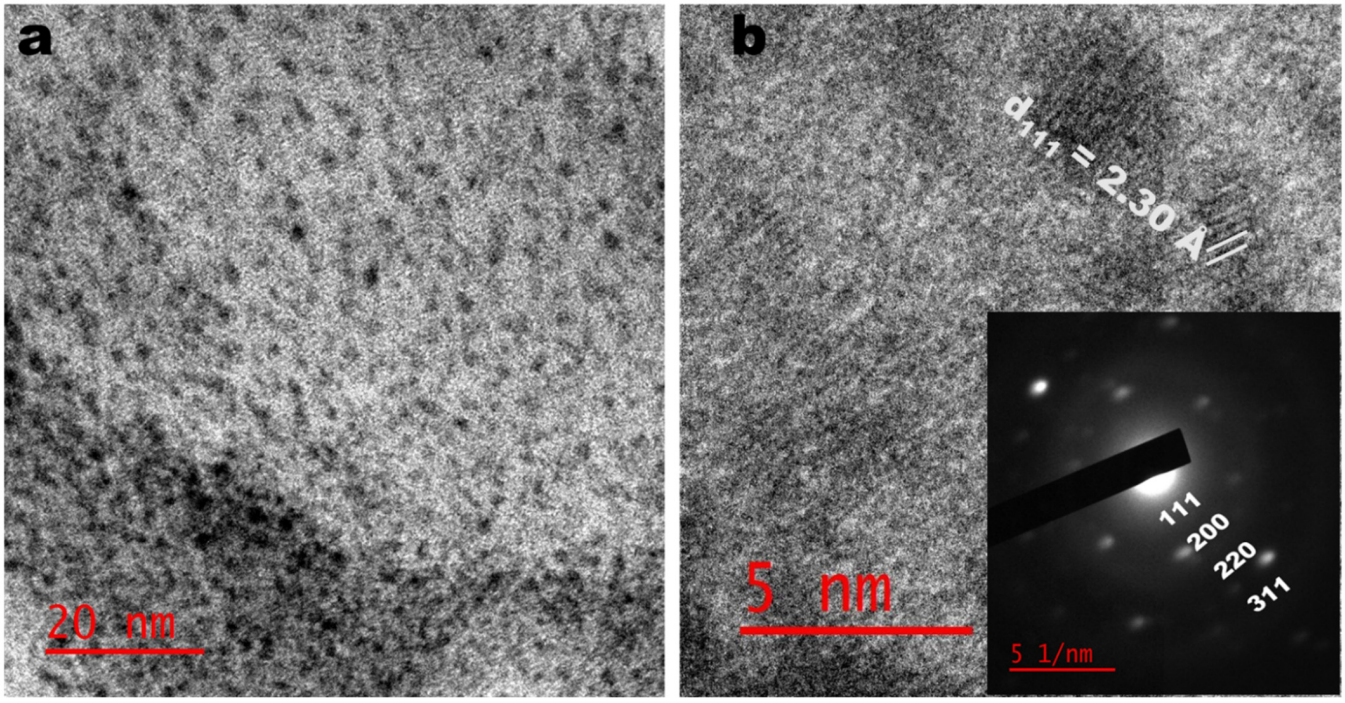

Figure 3. TEM (**a**) and HRTEM (**b**) images of CE synthesized PtNPs (Inset: SAED).

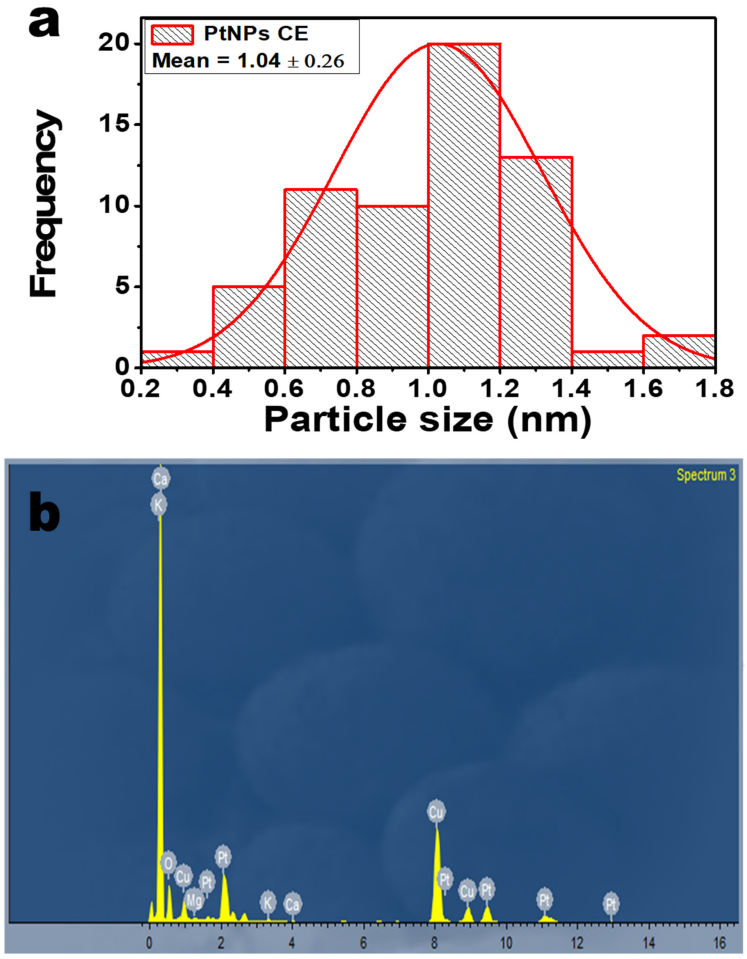

Figure 4. (**a**) Particle size distribution of PtNPs; (**b**) EDX spectra of PtNPs.

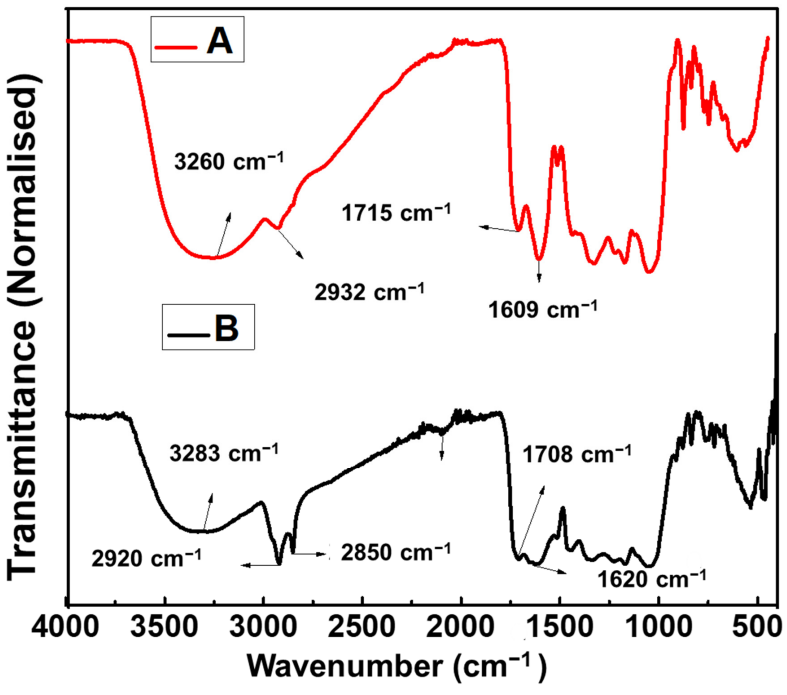

Figure 5. FTIR spectra of (**A**) CE extract, (**B**) PtNPs synthesized from CE extract.

Table 1. Assignment of IR bands for CE extract and as-synthesized PtNPs.

S.N.	CE Extract Vibrational Mode (cm^{-1})	PtNPs CE Vibrational Mode (cm^{-1})	Assignment
1	3260	3283	OH- Stretching
2	2932	2920, 2850	C-H Stretching
4	1715	1708	C=O Stretching
5	1609	1620	COO- Stretching
6	1515	1505	N-O Stretching
7	1440 1328	1443 1338	C-N Stretching of Aromatic Amine
8	1174	1170	S=O Stretching
9	1052	1057	C-O-C Stretching
10	837	835	C-H Bending
11	769	759	C-H Bending

2.5. Antibacterial Activity

The as-synthesized PtNPs were evaluated for antibacterial activities against diverse pathogenic Gram-positive (+ve) and Gram-negative (−ve) bacteria. The as-synthesized PtNPs exhibited inhibitory activity against the pathogenic bacteria at different concentrations, as shown in Supplementary Material Table S1. Figure 6 shows a graphical presentation of the MIC values of the PtNPs tested against the listed bacterial strains. Significantly, the as-synthesized PtNPs showed selectivity toward Gram-negative *Klebsiella* species of *Klebsiella aerogenes* and *Klebsiella oxytoca* at a very low MIC value of 1.56 µg/mL. *Staphylococcus epidermidis* and *Proteus mirabilis* showed susceptibility to the CE capped PtNPs but at a higher MIC value of 3.125 µg/mL. *Enterococcus faecalis*, *Bacillus subtilis*, and *Klebsiella pneumoniae* were susceptible at a much higher concentration, ranging from 500 to 2000 µg/mL. The PtNPs showed no inhibitory effect against *Escherichia coli*, *Staphylococcus aureus, Proteus vulgaris,* and *Mycobacterium smegmatis*. A preliminary study evaluating the antibacterial effect of the CE extract showed no effective inhibitory properties compared to the PtNPs (Supplementary Material Table S1). The observed low MIC value observed for the *Klebsiella* species of Ka and Ko could be due to oxidative stress as a result of reactive oxygen species (ROS) that are produced via a redox process. This eventually causes membrane and DNA damage that culminates in cell death. Cell death via ROS is often more potent [27]. A higher MIC value observed in *Klebsiella pneumoniae* can be attributed to the fact that it is one of the most virulent and resistant species of the *Klebsiella* genus. Such virulence factors are the production of hyper capsules, siderophores such as salmochelin and aerobactin, genetic codes for allantoin metabolism, and fimbriae [28,29]. All these are believed to contribute to the pathogenicity of *K. pneumoniae*, which possibly makes it less susceptible or resistant to ROS [29], and thus, a higher MIC value was obtained compared to the other *Klebsiella* species. Another plausible reason for the higher MIC values could be metal ion release. The metal ion interacts with the amine and carboxylic groups of proteins and nucleic acids to cause cell death. This is a less potent and slower mechanism, and thus, a larger amount of MNPs are required for cell death [27,30,31].

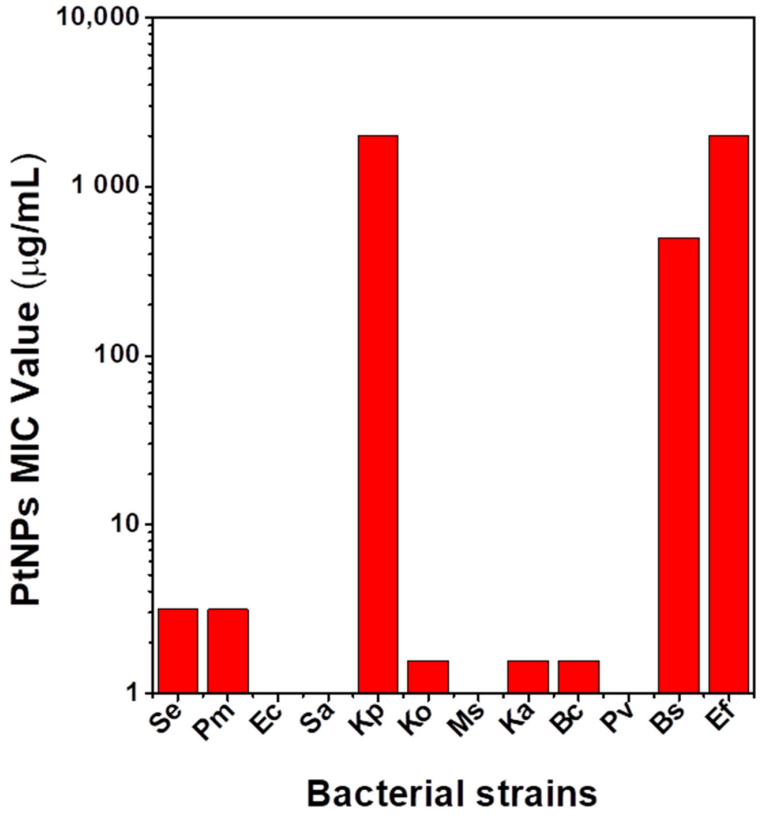

Figure 6. MIC values of PtNPs.

3. Materials and Methods

3.1. Materials

Analytical grade hexachloroplatinic (IV) acid hydrate ($H_2PtCl_6 \cdot xH_2O$) and Mueller–Hinton agar and broth were procured from Sigma-Aldrich, South Africa. One mg/mL streptomycin was purchased from Sigma Aldrich, St. Gallen, Switzerland (BCBP5897V). All aqueous solutions were prepared using deionized water.

3.2. Preparation of the Plant Extract

Healthy CE leaves were obtained from the Water Sisulu National Botanical Garden at Roodepoort, Johannesburg. The leaves were cleaned and afterwards dried under ambient conditions. Five grams of the dried leaves were mixed with 100 mL of deionized water and heated at 90 °C for 1 h. The mixture was filtered using a Whatman filter paper, and the filtrate was used for the synthesis.

3.3. Green synthesis of PtNPs

First, 10 mL of the extract from the CE leaf was added to 50 mL of 1 mM $H_2PtCl_6 \cdot xH_2O$ at 85 °C under reflux at a stirring rate of 750 rpm for 24 h.

3.4. Characterization

A Perkin Elmer Lambda 25 UV-Vis spectrophotometer was used for the absorption measurement. The absorption spectra were recorded in the range of 200–700 nm. The shape and size of the as-synthesized PtNPs were determined by transmission electron microscopy (TEM) using JEOL JEM-2100 at an acceleration voltage of 200 kV. The zeta potential analysis of the PtNPs was studied at 25 °C using Malvern Panalytical Zetasizer Nano ZS based on the Smoluchowski model. The surface chemistry of the sample was investigated using Perkin Elmer Spectrum Two FTIR spectroscopy over the range of 4000–400 cm^{-1}. X-ray diffraction (XRD) studies were conducted with monochromatic Cu-

Kα1 radiation (λ = 1.54 Å) at the diffraction angle range of 10° and 90° using a Bruker D8 Advance X-ray diffractometer.

3.5. Antibacterial Activity of PtNPs

The microdilution technique was used in the evaluation of the MIC. Fresh bacterial growths of the listed pathogenic bacteria strains (*Staphylococcus epidermidis* (Se) (ATCC14990), Proteus *mirabilis* (Pm), (ATCC 7002), *Escherichia coli* (Ec) (ATCC 25922), *Enterococcus faecalis* (Ef) (ATCC 13047), *Bacillus subtilis* (Bs) (ATCC 19659), *Staphylococcus aureus (Sa) (ATCC 25923), Klebsiella pneumoniae (Kp) (ATCC 13822), Klebsiella oxytoca (Ko) (ATCC 8724), Mycobacterium smegmatis (Ms) (MC 2155), Bacillus cereus (Bc) (ATCC 10876)*, and *Klebsiella aerogenes* (Ka) (ATCC 27853)] were standardized to the 0.5 McFarland standards in Muller–Hilton broth, which was then used as inoculum. In 96-well plate containing 100 µL of 2000, 1000, 500, 250, 125, 62.5, 50, 25, 12.5, 6.25, 3.125 and 1.56 µg/mL of PtNPs; 100 µL of each inoculum were seeded in triplicate. The plates were grown overnight at 37 °C. Muller–Hilton broth (50% *v/v* in DMSO) was used as a negative control. Streptomycin (1 mg/mL) served as the positive control. Viable cells were confirmed in the presence of resazurin dye after 2 h incubation as they enzymatically reduced resazurin dye (blue color) to the resorufin that fluoresces pink. A pink color indicates bacterial growth. The smallest concentration that inhibited bacterial growth was recorded as the MIC, and the values were recorded for each bacteria strain.

4. Conclusions

A simple, cost-effective, green, and eco-friendly method was used to synthesize water-soluble CE stabilized PtNPs. The leaf extract *of Combretum erythrophyllum* served as the bio-reductant and stabilizing agent. An optical characterization by UV-Vis was used to confirm the formation of the PtNPs. XRD studies revealed the formation of PtNPs with a cubic crystal structure, while the FTIR study confirmed the role of the biomolecules of CE extract as a capping agent in the biosynthesis of the PtNPs. The CE capped PtNPs are spherical in shape with an average particle diameter of 1.04 ± 0.26 nm. The biosynthesized PtNPs showed selective inhibition toward Gram-negative Klebsiella species implicated in nosocomial infections. This study could serve as a starting point in exploring CE-capped PtNPs in nanomedicine for the treatment of nosocomial infectious diseases.

Supplementary Materials: The following are available online at https://www.mdpi.com/article/10.3390/antibiotics10111275/s1, Table S1: Antibacterial study of PtNPs, CE extract and streptomycin via minimum inhibitory concentration method.

Author Contributions: Conceptualization, O.S.O.; methodology, O.S.O. and O.T.F.; validation, O.T.F. and O.S.O.; formal analysis, O.T.F., S.P., R.M., T.C.L., N.M. and R.J.V.; investigation, O.T.F.; resources, O.S.O.; data curation, O.T.F. and O.S.O.; writing—original draft preparation, O.T.F.; writing—review and editing, O.S.O.; visualization, O.S.O. and O.T.F.; supervision, O.S.O. and V.M.; project administration and funding acquisition, O.S.O. All authors have read and agreed to the published version of the manuscript.

Funding: National Research Foundation (N.R.F) under the Competitive Programme for Rated Researchers (CPRR), grant no 129290, and the University of Johannesburg research committee (URC) and Faculty of Science research committee (FRC).

Data Availability Statement: The data presented in this study are available in this manuscript and Supplementary Material.

Acknowledgments: The authors would like to thank National Research Foundation (N.R.F) under the Competitive Programme for Rated Researchers (CPRR), the University of Johannesburg research committee (URC) and the Faculty of Science research committee (FRC) for their financial support. The authors would also like to thank Christopher Willis, Andrew Hankey, and Solomon Nenungwi of the Walter Sisulu National Botanical Garden, Roodepoort, for their provision of the plant.

Conflicts of Interest: The authors declare no conflict of interest.

References

1. Jameel, M.S.; Aziz, A.A.; Dheyab, M.A. Green synthesis: Proposed mechanism and factors influencing the synthesis of platinum nanoparticles. *Green Process. Synth.* **2020**, *9*, 386–398. [CrossRef]
2. Şahin, B.; Aygün, A.; Gündüz, H.; Şahin, K.; Demir, E.; Akocak, S.; Şen, F. Cytotoxic effects of platinum nanoparticles obtained from pomegranate extract by the green synthesis method on the MCF-7 cell line. *Colloids Surf. B Biointerfaces* **2018**, *163*, 119–124. [CrossRef]
3. Ansari, M.A.; Kalam, A.; Al-Sehemi, A.G.; Alomary, M.N.; AlYahya, S.; Aziz, M.K.; Srivastava, S.; Alghamdi, S.; Akhtar, S.; Almalki, H.D.; et al. Counteraction of Biofilm Formation and Antimicrobial Potential of Terminalia catappa Functionalized Silver Nanoparticles against Candida albicans and Multidrug-Resistant Gram-Negative and Gram-Positive Bacteria. *Antibiotics* **2021**, *10*, 725. [CrossRef]
4. Jemilugba, O.T.; Sakho, E.H.M.; Parani, S.; Mavumengwana, V.; Oluwafemi, O.S. Green synthesis of silver nanoparticles using Combretum erythrophyllum leaves and its antibacterial activities. *Colloids Interface Sci. Commun.* **2019**, *31*, 100191. [CrossRef]
5. Azharuddin, M.; Zhu, G.H.; Das, D.; Ozgur, E.; Uzun, L.; Turner, A.P.F.; Patra, H.K. A repertoire of biomedical applications of noble metal nanoparticles. *Chem. Commun.* **2019**, *55*, 6964–6996. [CrossRef]
6. Aygun, A.; Gülbagca, F.; Ozer, L.Y.; Ustaoglu, B.; Altunoglu, Y.C.; Baloglu, M.C.; Atalar, M.N.; Alma, M.H.; Sen, F. Biogenic platinum nanoparticles using black cumin seed and their potential usage as antimicrobial and anticancer agent. *J. Pharm. Biomed. Anal.* **2020**, *179*, 112961. [CrossRef] [PubMed]
7. Pedone, D.; Moglianetti, M.; De Luca, E.; Bardi, G.; Pompa, P.P. Platinum nanoparticles in nanobiomedicine. *Chem. Soc. Rev.* **2017**, *46*, 4951–4975. [CrossRef]
8. Borse, V.; Kaler, A.; Banerjee, U.C. Microbial Synthesis of Platinum Nanoparticles and Evaluation of Their Anticancer Activity. *Int. J. Emerg. Trends Electr. Electron.* **2015**, *11*, 26–31. [CrossRef]
9. Tahir, K.; Nazir, S.; Ahmad, A.; Li, B.; Khan, A.U.; Khan, Z.U.H.; Khan, F.U.; Khan, Q.U.; Khan, A.; Rahman, A.U. Facile and green synthesis of phytochemicals capped platinum nanoparticles and in vitro their superior antibacterial activity. *J. Photochem. Photobiol. B Biol.* **2017**, *166*, 246–251. [CrossRef] [PubMed]
10. John Leo, A.; Oluwafemi, O.S. Plant-mediated synthesis of platinum nanoparticles using water hyacinth as an efficient biomatrix source-An eco-friendly development. *Mater. Lett.* **2017**, *196*, 141–144. [CrossRef]
11. Deng, H.H.; Lin, X.L.; Liu, Y.H.; Li, K.L.; Zhuang, Q.Q.; Peng, H.P.; Liu, A.L.; Xia, X.H.; Chen, W. Chitosan-stabilized platinum nanoparticles as effective oxidase mimics for colorimetric detection of acid phosphatase. *Nanoscale* **2017**, *9*, 10292–10300. [CrossRef] [PubMed]
12. Jeyaraj, M.; Gurunathan, S.; Qasim, M.; Kang, M.H.; Kim, J.H. A comprehensive review on the synthesis, characterization, and biomedical application of platinum nanoparticles. *Nanomaterials* **2019**, *9*, 1719. [CrossRef] [PubMed]
13. Nazir, A. A review: Use of plant extracts and their phytochemical constituents to control antibiotic resistance in S. aureus. *Pure. Appl. Biol.* **2020**, *9*, 720–727. [CrossRef]
14. Khin, M.; Jones, A.M.; Cech, N.B.; Caesar, L.K. Phytochemical analysis and antimicrobial efficacy of macleaya cordata against extensively drug-resistant Staphylococcus aureus. *Nat. Prod. Commun.* **2018**, *13*, 1934578X1801301117. [CrossRef] [PubMed]
15. Hussein, R.A.; El-Anssary, A.A. Plants Secondary Metabolites: The Key Drivers of the Pharmacological Actions of Medicinal Plants. *Herb. Med.* **2019**, *1*, 3. [CrossRef]
16. Santhoshkumar, J.; Rajeshkumar, S.; Venkat Kumar, S. Phyto-assisted synthesis, characterization and applications of gold nanoparticles-A review. *Biochem. Biophys. Rep.* **2017**, *11*, 46–57. [CrossRef] [PubMed]
17. Khoshnamvand, M.; Ashtiani, S.; Huo, C.; Saeb, S.P.; Liu, J. Use of Alcea rosea leaf extract for biomimetic synthesis of gold nanoparticles with innate free radical scavenging and catalytic activities. *J. Mol. Struct.* **2019**, *1179*, 749–755. [CrossRef]
18. Wei, S.; Wang, Y.; Tang, Z.; Hu, J.; Su, R.; Lin, J.; Zhou, T.; Guo, H.; Wang, N.; Xu, R. A size-controlled green synthesis of silver nanoparticles by using the berry extract ofSea Buckthornand their biological activities. *New J. Chem.* **2020**, *44*. [CrossRef]
19. Nishanthi, R.; Malathi, S.; John, P.S.; Palani, P. Green synthesis and characterization of bioinspired silver, gold and platinum nanoparticles and evaluation of their synergistic antibacterial activity after combining with different classes of antibiotics. *Mater. Sci. Eng. C* **2019**, *96*, 693–707. [CrossRef]
20. Kumar, P.V.; Jelastin Kala, S.M.; Prakash, K.S. Green synthesis derived Pt-nanoparticles using Xanthium strumarium leaf extract and their biological studies. *J. Environ. Chem. Eng.* **2019**, *7*, 103146. [CrossRef]
21. Bantho, S.; Naidoo, Y.; Dewir, Y.H. The secretory scales of Combretum erythrophyllum (Combretaceae): Micromorphology, ultrastructure and histochemistry. *South Afr. J. Bot.* **2020**, *131*, 104–117. [CrossRef]
22. Martini, N.; Eloff, J.N. The preliminary isolation of several antibacterial compounds from Combretum erythrophyllum (Combretaceae). *J. Ethnopharmacol.* **1998**, *62*, 255–263. [CrossRef]
23. Manzoor, S.; Bashir, D.J.; Imtiyaz, K.; Rizvi, M.M.A.; Ahamad, I.; Fatma, T.; Agarwal, N.B.; Arora, I.; Samim, M. Biofabricated platinum nanoparticles: Therapeutic evaluation as a potential nanodrug against breast cancer cells and drug-resistant bacteria. *RSC Adv.* **2021**, *11*, 24900–24916. [CrossRef]
24. Demir, E.; Savk, A.; Sen, B.; Sen, F. A novel monodisperse metal nanoparticles anchored graphene oxide as Counter Electrode for Dye-Sensitized Solar Cells. *Nano-Struct. Nano-Objects* **2017**, *12*, 41–45. [CrossRef]
25. He, K.; Chen, N.; Wang, C.; Wei, L.; Chen, J. Method for Determining Crystal Grain Size by X-ray Diffraction. *Cryst. Res. Technol.* **2018**, *53*, 1700157. [CrossRef]

26. Fanoro, O.T.; Parani, S.; Maluleke, R.; Lebepe, T.C.; Varghese, J.R.; Mavumengwana, V.; Oluwafemi, O.S. Facile Green, Room-Temperature Synthesis of Gold Nanoparticles Using Combretum erythrophyllum Leaf Extract: Antibacterial and Cell Viability Studies against Normal and Cancerous Cells. *Antibiotics* **2021**, *10*, 893. [CrossRef] [PubMed]
27. Harun, A.M.; Noor, N.F.M.; Zaid, A.; Yusoff, M.E.; Shaari, R.; Affandi, N.D.N.; Fadil, F.; Rahman, M.A.A.; Alam, M.K. The Antimicrobial Properties of Nanotitania Extract and Its Role in Inhibiting the Growth of Klebsiella pneumonia and Haemophilus influenza. *Antibiotics* **2021**, *10*, 961. [CrossRef] [PubMed]
28. Wyres, K.L.; Lam, M.M.C.; Holt, K.E. Population genomics of Klebsiella pneumoniae. *Nat. Rev. Microbiol.* **2020**, *18*, 344–359. [CrossRef]
29. Paczosa, M.K.; Mecsas, J. Klebsiella pneumoniae: Going on the Offense with a Strong Defense. *Microbiol. Mol. Biol. Rev.* **2016**, *80*, 629–661. [CrossRef] [PubMed]
30. Hussein-Al-Ali, S.H.; El Zowalaty, M.E.; Hussein, M.Z.; Geilich, B.M.; Webster, T.J. Synthesis, characterization, and antimicrobial activity of an ampicillin-conjugated magnetic nanoantibiotic for medical applications. *Int. J. Nanomed.* **2014**, *9*, 3801. [CrossRef] [PubMed]
31. Regmi, C.; Joshi, B.; Ray, S.K.; Gyawali, G.; Pandey, R.P. Understanding Mechanism of Photocatalytic Microbial Decontamination of Environmental Wastewater. *Front. Chem.* **2018**, *6*, 33. [CrossRef] [PubMed]